

---

# Fast Heterogeneous Federated Learning with Hybrid Client Selection

---

Guangyuan Shen<sup>1,2</sup>, Dehong Gao<sup>\*2</sup>, Duanxiao Song<sup>1</sup>, Libin Yang<sup>†1</sup>, Xukai Zhou<sup>1</sup>, Shirui Pan<sup>3</sup>, Wei Lou<sup>4</sup>, and Fang Zhou<sup>1</sup>

<sup>1</sup>Department of Cyber Science and Technology, Northwestern Polytechnical University, China

<sup>2</sup>Alibaba Group, China

<sup>3</sup>Department of Data Science and AI, Faculty of IT, Monash University, Australia

<sup>4</sup>Department of Computing, The Hong Kong Polytechnic University, Hong Kong, China

{gyshen, songduanxiao, libiny, zhouxukai, zhoufang}@mail.nwpu.edu.cn, dehong.gdh@alibaba-inc.com, shirui.pan@monash.edu, csweilou@comp.polyu.edu.hk

## Abstract

Client selection schemes are widely adopted to handle the communication-efficient problems in recent studies of Federated Learning (FL). However, the large variance of the model updates aggregated from the randomly-selected unrepresentative subsets directly slows the FL convergence. We present a novel clustering-based client selection scheme to accelerate the FL convergence by variance reduction. Simple yet effective schemes are designed to improve the clustering effect and control the effect fluctuation, therefore, generating the client subset with certain representativeness of sampling. Theoretically, we demonstrate the improvement of the proposed scheme in variance reduction. We also present the tighter convergence guarantee of the proposed method thanks to the variance reduction. Experimental results confirm the exceed efficiency of our scheme compared to alternatives.

## 1 Introduction

Federated Learning (FL) is a distributed learning paradigm for training a global model from data scattered across different clients [14]. During the training process, all the clients need to operate data locally and transfer the model updates between servers and themselves back and forth. Such a training process may raise many challenges, with communication cost often being the critical bottleneck [10].

Many studies have found that different clients might transfer similar (or redundant) model updates to the server, which is a waste of communication costs [1, 6, 11]. Client selection schemes are widely adopted to reduce the waste of communication costs, e.g., Federated Averaging (FedAvg) where only the randomly-selected subset of clients transfer their model update to the server instead of yielding all clients involved [19]. FedAvg can maintain the learning efficiency with reduced communication costs, since the random selection schemes can reduce the redundant update transmission. When FedAvg meets client sets with low similarity, the server can not accurately pick out the representative clients. The large variance of the update gradient aggregated from the unrepresentative subset directly slows the training convergence [6, 12].

To accelerate the training convergence by variance reduction, many client selection criteria have been proposed in recent literature, e.g., importance sampling, where the probabilities for clients to be

---

\*The first and second author contribute equally to this work.

†Contact Author

selected is proportional to their importance measured by the norm of update [3], data variability [22], and test accuracy [20]. However, importance sampling could not effectively capture the similarities among the clients. As shown in Figure 1(a), applying importance sampling could cause learning inefficiency as the clients transfer excessive important yet similar updates to the server. To make better use of the similarities among clients, some researchers propose raw gradient-based cluster sampling schemes that group the clients with similar gradient together [6, 21], shown in Figure 1(b). If the clustering effect is good enough, cluster sampling can easily pick out the representative clients. Unfortunately, the effect of raw gradient-based clustering methods faces the following problems: (i) **Poor Effect**, the high dimension gradient of a client is too complicated to be an appropriate cluster feature, which can not bring a good clustering effect. (ii) **Effect Fluctuation**, due to the limitations of the clustering algorithm, when operating the client set with different parameters settings, e.g., different numbers of clusters, the clustering effect tends to fluctuate greatly. After clustering with poor and fluctuant effect, there always exists some clusters with low client similarity. Applying client selection in the clusters with low client similarity may slow the overall training convergence. Besides, both the importance and cluster sampling methods require all the clients to return the raw gradient information for better selection, which runs against the communication reduction objective.

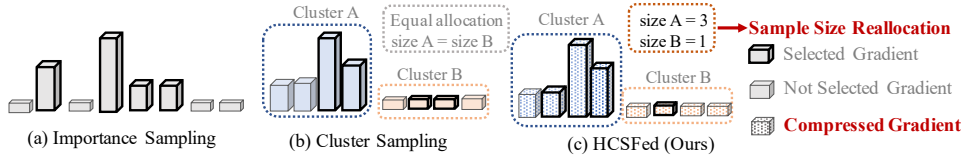


Figure 1: The differences among client selection schemes. The heights represent the norm of the gradients. The different colors denote different clusters. We highlight the main difference by red bold font.

We propose **HCSFed**, a novel **Hybrid Clustering-based client Selection** scheme for heterogeneous **Federated** learning that further accelerates the FL convergence. To improve the **poor clustering effect**, different from using the high dimension gradient, we adopt the compressed gradient as the cluster feature. The different components of the gradient are grouped based on their numerical value, only the center of the group are retained to form the compressed gradient. Adopting the compressed gradient as cluster feature not only allows better clustering effect but also is communication-efficient, since the compression operation filters out the redundant information within each gradient. Besides, to control the **effect fluctuation**, we reset the number of clients to be selected in each cluster based on the client similarity and the size of the cluster, which we term as sample size re-allocation. As shown in Figure 1(c), sample size re-allocation scheme makes the cluster with low similarity have more number of clients to be selected. The sampling effect becomes stable because the poor effect of random sampling in the clusters with low similarity is greatly mitigated by sample size re-allocation scheme. Theoretically, we demonstrate the improvement of the proposed scheme in variance reduction. Extensive experiments show the exceed efficiency of the proposed scheme compared to the cutting-edge FL client selection criteria in both convex and non-convex settings.

## 2 System Setup and Prior Work

**The Federated Learning Optimization Settings.** In federated learning, a total number of  $N$  clients aim to jointly solve the following distributed optimization model:

$$\min_{\mathbf{w} \in \mathbb{R}^d} \left\{ F(\mathbf{w}) := \sum_{k=1}^N \omega_k \left( F_k(\mathbf{w}) := \frac{1}{n_k} \sum_{j=1}^{n_k} f(\mathbf{w}; x_{k,j}) \right) \right\}, \quad (1)$$

where  $\omega_k$  is the weight of the  $k^{th}$  client, *s.t.*  $\omega_k \geq 0$  and  $\sum_{k=1}^N \omega_k = 1$ . Suppose the  $k^{th}$  client possesses  $n_k$  training data:  $\{x_{k,1}, x_{k,2}, \dots, x_{k,n_k}\}$ . The local objective function  $F_k(\mathbf{w})$  is defined as the average of  $f(\mathbf{w}; x_{k,j})$ , which is a user-specified loss function (possibly non-convex) made with model parameters  $\mathbf{w} \in \mathbb{R}^d$  and training data  $x_{k,j}$ .

**FedAvg Description.** In the  $t^{th}$  train round of the FedAvg, the server broadcasts the latest global model  $\mathbf{w}_t$  to all the clients. The  $k^{th}$  client sets  $\mathbf{w}_t^k \leftarrow \mathbf{w}_t$  and performs local training for  $E$  epochs:

$$\mathbf{w}_{t+1}^k \leftarrow \mathbf{w}_t^k - \eta_t \nabla F_k(\mathbf{w}_t^k, \xi_t^k), \quad (2)$$

where  $\eta_t$  is the learning rate and  $\xi_t^k$  is a data sample uniformly selected from the local data. In the communication round, the server aggregates the local model update to produce the new global model  $\mathbf{w}_{t+E}$ . In fact, to reduce the communication cost,  $\text{FedAvg}$  randomly generates a subset  $\mathcal{S}_t$  consisting of  $m$  clients from the entire client set and aggregates the model update,  $\{\mathbf{w}_{t+E}^1, \mathbf{w}_{t+E}^2, \dots, \mathbf{w}_{t+E}^m\}$ ,

$$\mathbf{w}_{t+E} \leftarrow \underbrace{\sum_{k=1}^N \omega_k \mathbf{w}_{t+E}^k}_{\text{Full Participate}} \leftarrow \underbrace{\sum_{k \in \mathcal{S}_t} \frac{N}{m} \omega_k \mathbf{w}_{t+E}^k}_{\text{Partial Participate}}. \quad (3)$$

LAG [2] is a improved aggregation scheme where it triggers the reuse of outdated gradients for the non-selected clients, but the variance of the aggregated gradient is still large, which directly slows the FL convergence. To accelerate the convergence by variance reduction, many client selection criteria have been proposed in recent literature, including importance-based and clustering-based methods.

**Importance Sampling.** Importance sampling is a non-uniform client selection method, where the probabilities for clients to be chosen are proportional to their importance [12, 29]. Different methods to measure the importance are proposed, including data variability [22], norm of update [3], test accuracy [20], local rounds [23], and local loss [4]. Such methods can yield better selection by activating the clients with more importance. However, they could not capture the similarities among the updates of clients and, therefore, trigger the communication redundancy.

**Cluster Sampling.** To make better use of similarities among clients, some researchers propose raw gradient-based cluster sampling schemes that group the clients with similar gradients together [6, 21]. However, the effect of cluster sampling strongly relies on the performance of the clustering process. Unfortunately, the high dimension gradient of a client is too complicated to be an appropriate cluster feature, which can not bring a good clustering effect. Besides, meticulous one-by-one client selection [1, 5] is introduced to FL. It could achieve better selection outcomes but with extra expensive computation and communication costs for solving each noncommittal submodular maximization.

**Difference from SCAFFOLD.** While SCAFFOLD [11] appears to be similar to our method, there are fundamental differences. SCAFFOLD augments the updates with extra ‘‘control-variate’’ item that is also transmitted along with the updates to reduce the variance, while we reduce the variance by selecting a more representative subset. The former focuses on update control, while the latter focuses on better update selection, indicating that they are orthogonal and compatible with each other.

### 3 HCSFed: Proposed Client Selection Scheme in Federated Learning

#### 3.1 Analysis for the Optimization Objective of Client Selection Scheme

Inspired by the convergence analysis work [12], we define the convergence speed as follows,

$$\begin{aligned} \text{Speed} &\triangleq -\mathbb{E} \left[ \|\mathbf{w}_{t+1} - \mathbf{w}^*\|_2^2 - \|\mathbf{w}_t - \mathbf{w}^*\|_2^2 \right] \\ &= -\mathbb{E} \left[ (\mathbf{w}_t - \eta_t \nabla F_k)^T (\mathbf{w}_t - \eta_t \nabla F_k) + 2\eta_t \nabla F_k^T \mathbf{w}^* - \mathbf{w}_t^T \mathbf{w}_t \right] \\ &= \underbrace{2\eta_t (\mathbf{w}_t - \mathbf{w}^*) \mathbb{E}[G_t] - \eta_t^2 \mathbb{E}[G_t]^T \mathbb{E}[G_t]}_{\text{Constant}} - \underbrace{\eta_t^2 \text{Tr}(\mathbb{V}[G_t])}_{\text{Changeable}}, \end{aligned} \quad (4)$$

where  $G_t = \nabla F(\mathbf{w}_t, \mathcal{S}_t)$  and  $\mathbb{E}[G_t] = \sum_{k=1}^N \nabla F_k(\mathbf{w}_t^k, x^k)$  is the unbiased estimate of the true update. The first two terms are constant, since  $\mathbb{E}[G_t]$  has a constant value. Therefore, gaining a convergence speedup is equivalent to reducing the variance of gradient, i.e.,  $\mathbb{V}[G_t]$ . Consider a partial participation FL [17], selecting  $m$  clients can be regarded as selecting one client  $m$  times by  $m$  different discrete probability distributions  $\{P_i\}_{i=1}^m$ . For each distribution, we have  $P_i = \{p_k^i\}_{k=1}^N$ , where  $p_k^i$  denotes the probability for the  $k^{\text{th}}$  client to be selected in  $i^{\text{th}}$  distribution. For faster convergence, we seek to minimize the variance of model update  $\mathbf{w}(\mathcal{S}_t)$  aggregated from the subset that is equivalent to minimizing the variance of gradient corresponding to the following equation:

$$\min_{p_k^i} \{ \mathbb{V}[G_t] = \mathbb{V}[\mathbf{w}(\mathcal{S}_t)] \}, \text{ s.t., } \sum_{k=1}^N p_k^i = 1 \text{ with } p_k^i \geq 0, \|\mathcal{S}_t\| = q \cdot N = m, \quad (5)$$

where we use  $q$  and  $N$  to denote the sampling ratio and the total number of all clients, respectively.

### 3.2 Proposed Client Selection Scheme HCSFed for Variance Reduction

How to explore and make use of the similarities among clients with acceptable resource costs is the key issue in constructing client selection criteria. We propose HCSFed, a client selection scheme that exploits three components (cluster sampling, sample size re-allocation, importance sampling) guaranteeing convergence speedup by variance reduction.

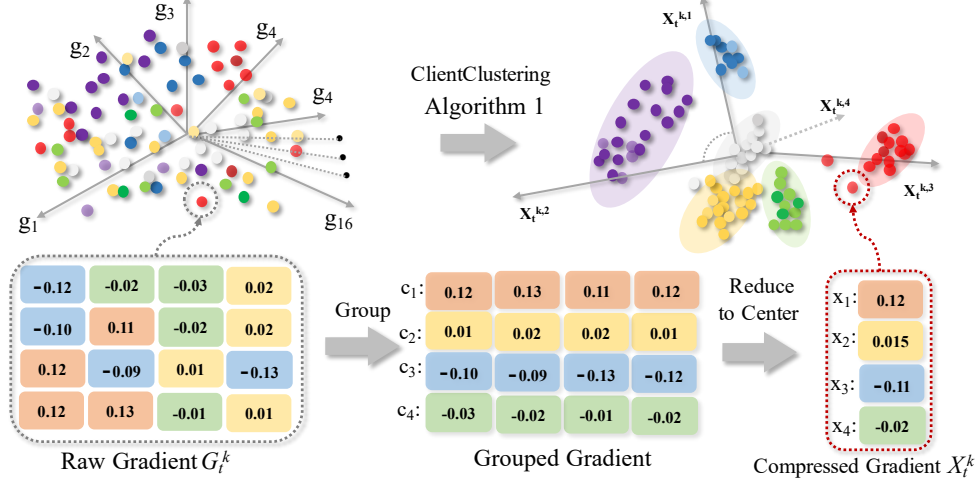


Figure 2: The visualizations of the raw gradient (left) and the clustered compressed gradient (right). Each point denotes the update gradient of one client. The  $g_i$  is the  $i^{th}$  component of the update gradient. The  $c_i$  denotes the  $i^{th}$  group of component.

**The Compressed Gradient-Based Cluster Selection.** To roughly explore and make use of the similarity among clients, we develop cluster selection that groups the similar clients together based on the client characteristic. The following is a mathematical description of cluster selection. Generating a subset  $S_t$  consisting of  $m$  clients by clustering selection can be regarded as selecting  $m$  clients using  $H$  different probability distributions  $\{P_h\}_{h=1}^H$  where  $P_h = \{p_k^h\}_{k=1}^N$ . For example, if we select a client from the  $h^{th}$  cluster, the probability distribution  $P_h$  will be used, and the  $p_k^h$  comes as follows:

$$p_k^h = \begin{cases} 0, & \text{if } k^{th} \text{ client} \notin h^{th} \text{ cluster} \\ \frac{1}{N_h}, & \text{if } k^{th} \text{ client} \in h^{th} \text{ cluster} \end{cases} \quad (6)$$

where  $N_h$  denotes the number of clients in the  $h^{th}$  cluster *s.t.*  $\sum_{h=1}^H N_h = N$ . Prior cluster selections [6] prefer to develop clustering based on the raw high dimension gradient (shown in Figure 2), which is too complicated to distinguish clients and brings unacceptable communication costs running against the original objective. Different from the previous raw gradient-based clustering methods, we develop clustering based on compressed gradient [9] which is the information-preserving representation of the model update. As shown in Figure 2, different components of the gradient are grouped based on their numerical value, only the center of the group are retained to form the compressed gradient. The compression rate  $R$  can be obtained by evaluating the quotient of  $d$  and  $d'$ , i.e.,  $\frac{d'}{d}$ , where  $d'$  and  $d$  are the total dimension of the compressed gradient and raw gradient, respectively. Adopting the compressed gradient as cluster feature not only allows better clustering effect but also is communication-efficient, since the compression operation filters out the redundant information within each gradient. The pseudo-code of Gradient Compress (GC) can be found in

#### Algorithm 1: ClientClustering

---

**Input:** compressed gradient of all the clients in the  $t^{th}$  round  $\{X_t^k\}_{k=1}^N$   
**Input:** The number of the clusters  $H$

- 1 **Initialize** Randomly select  $H$  clients as cluster centers  $\{\mu_1, \mu_2, \dots, \mu_H\}$ ;
- 2 **Initialize**  $C_i = \emptyset$  ( $1 \leq i \leq H$ );
- 3 **repeat**
- 4   **for each client**  $k=1, 2, \dots, N$  **do**
- 5      $\lambda_k = \arg \min_{i \in \{1, 2, \dots, H\}} \|X_t^k - \mu_i\|_2$ ;
- 6      $C_{\lambda_k} = C_{\lambda_k} \cup \{k^{th} \text{ client with } X_t^k\}$ ;
- 7   **end**
- 8   **for each cluster**  $i=1, 2, \dots, H$  **do**
- 9     New center  $\mu'_i = \frac{1}{|C_i|} \sum_{X_t^k \in C_i} X_t^k$ ;
- 10     $\mu_i \leftarrow \mu'_i$ ;
- 11   **end**
- 12 **until**  $\forall i = \{1, 2, \dots, H\}, \mu'_i = \mu_i$ ;

**Output:**  $\mathcal{G} = \{C_1, C_2, \dots, C_H\}$ ;

---

Appendix A.2. Algorithm 1 summarizes the main steps of client clustering. Ideally, after clustering, the clients in the same cluster are similar to each other. However, as shown in Figure 2, some clusters always exist with low similarity (purple cluster), since the effect of the clustering process fluctuates, which may also lead to performance degradation.

**Sample Size Re-allocation Scheme.** Concentrating on the diverse heterogeneity of clusters, we make the first attempt to develop a sample size re-allocation scheme that pays more attention to the cluster with great heterogeneity. HCSFed re-determines the sample size  $m_h$ , namely, the number of clients sampled from the  $h^{\text{th}}$  cluster, by considering both the cluster size  $N_h$  and variability.

$$m_h = \frac{N_h S_h}{\sum_{h=1}^H N_h S_h} \cdot m,$$

where  $S_h = \frac{1}{N_h - 1} \sum_{j=1, i \neq j}^{N_h} \|X_t^i - X_t^j\|_2^2$ ,

(7)

$m_h$  denotes the number of clients in the subset  $\mathcal{S}_t$  from the  $h^{\text{th}}$  cluster *s.t.*  $\sum_{h=1}^H m_h = m$ .  $S_h$  denotes the variability of the  $h^{\text{th}}$  cluster where we use Cluster Cohesion based on the compressed model update to approximate. The introduction of sample size re-allocation can further reduce the variance by assigning more sample chance to those clusters with greater heterogeneity. Due to the limited number of clients to be selected, sometimes some clusters with great heterogeneity still can not have an adequate sample chance, which indeed need extra care.

**Importance Selection.** We introduce importance selection to optimize the probabilities for clients to be selected in the same cluster, which is based on the norm of the compressed gradient, i.e.,  $\text{GC}(G_t^k) = X_t^k$ . We re-determine the probability for each client to be sampled in  $t^{\text{th}}$  round as follows,

$$p_t^k = \frac{\|\text{GC}(G_t^k)\|}{\sum_{k=1}^{N_h} \|\text{GC}(G_t^k)\|} = \frac{\|X_t^k\|}{\sum_{k=1}^{N_h} \|X_t^k\|}, \text{ if } k^{\text{th}} \text{ client} \in h^{\text{th}} \text{ cluster in } t^{\text{th}} \text{ round.} \quad (8)$$

After completing the importance selection, the client with a higher norm of gradient (more importance) will have a higher probability to be sampled, which brings representative outcomes under an inadequate sampling ratio. Importance selection provides a fine-grained optimization over cluster selection with sample size re-allocation, i.e., assigning more attention to the more representative clients.

These three ideas of selection discussed in this subsection together constitute the HCSFed scheme to optimize the client selection in FL. HCSFed selects representative clients via allocating appropriate probability for each client to be selected, with the promise of reducing the variance between the model update aggregated from the sampled subset  $\mathcal{S}_t$  and the entire set  $\mathcal{K}$ . As we mentioned in Section 3.1, the reduced variance leads to faster convergence. Therefore, HCSFed can achieve communication cost reduction, as it requires fewer rounds to approach the target accuracy. Algorithm 2 summarizes the main steps of HCSFed.

---

**Algorithm 2:** HCSFed

---

**Input:** updates in the  $t^{\text{th}}$  round of all clients  $\{G_t^k\}_{k=1}^N$

- 1 **Initialize**  $\mathbf{w}_0$ ;
- 2 **Initialize**  $\mathcal{S}_t = \emptyset$ ;
- 3 **Server executes:**
- 4 **for each round**  $t = 1, 2, \dots$  **do**
- 5      $m \leftarrow \max(qN, 1)$ ;
- 6      $\mathcal{G} \leftarrow \text{ClientClustering}(\mathbf{X}_t, \mathbf{H})$ ;
- 7     **for each cluster**  $h = 1, 2, \dots, H$  **do**
- 8          $m_h \leftarrow \frac{N_h S_h}{\sum_{h=1}^H N_h S_h} \cdot m$ ;
- 9         compute  $\{p_t^k\}_{k \in N_h}$  using Equation 8;
- 10          $\mathcal{S}_t = \mathcal{S}_t \cup m_h$  clients selected with  $P_h$ ;
- 11     **end**
- 12     **for client**  $\in \mathcal{S}_t$  **in parallel do**
- 13          $\mathbf{w}_{t+1}^k \leftarrow \text{ClientUpdate}(k, \mathbf{w}_t^k)$ ;
- 14     **end**
- 15      $\mathbf{w}_{t+1} \leftarrow \sum_{k \in \mathcal{S}_t} \frac{N}{m} \omega_k \mathbf{w}_{t+1}^k$ ;
- 16 **end**
- 17 **ClientUpdate**( $k, \mathbf{w}_t^k$ ):
- 18 **for each local epoch**  $i$  **from 1 to E do**
- 19      $\mathbf{w}_{t+i+1}^k \leftarrow \mathbf{w}_{t+i}^k - \eta \nabla F_k(\mathbf{w}_{t+i}^k, \xi_{t+i}^k)$ ;
- 20 **end**
- 21 **if**  $k \in \mathcal{S}_t$  **then**
- 22     **return**  $\mathbf{w}_{t+1}^k \leftarrow \mathbf{w}_{t+E}^k, X_t^k \leftarrow \text{GC}(G_t^k)$ ;
- 23 **else**
- 24     **return**  $X_t^k \leftarrow \text{GC}(G_t^k)$ ;
- 25 **end**

---

## 4 Theoretical Analysis

### 4.1 Variance Relationship among Different Selection Schemes

**Theorem 1** (Variance Reduction). *If the population is large compared to the subset,  $\frac{m}{N}$ ,  $\frac{m_h}{N_h}$ ,  $\frac{1}{m_h}$  and  $\frac{1}{N}$  are negligible, then the selection (or cross-client) variance of different selection schemes satisfies*

$$\mathbb{V}(\mathbf{w}_{\text{hybrid}}) \leq \mathbb{V}(\mathbf{w}_{\text{cldiv}}) \leq \mathbb{V}(\mathbf{w}_{\text{cluster}}) \leq \mathbb{V}(\mathbf{w}_{\text{rand}}),$$

where  $\mathbf{w}_{\text{hybrid}}$ ,  $\mathbf{w}_{\text{cldiv}}$ ,  $\mathbf{w}_{\text{cluster}}$ ,  $\mathbf{w}_{\text{rand}}$  denote the model update aggregated from the subset  $\mathcal{S}_t$  that generated by HCSFed, clustering selection scheme under re-allocation, clustering selection scheme under plain allocation and simple random selection scheme, respectively.

**Proof Sketch.** Below we provide a proof sketch to reveal the relationship among the cross-client variance of different client selection schemes, and then we naturally state when our HCSFed scheme could achieve variance reduction. We defer the details of proof to Appendix B.

**Comparison of Random and Clustering Selection.** We derive the Equation 9 to show the relationship between  $\mathbb{V}(\mathbf{w}_{\text{cluster}})$  and  $\mathbb{V}(\mathbf{w}_{\text{rand}})$ :

$$\mathbb{V}(\mathbf{w}_{\text{rand}}) = \mathbb{V}(\mathbf{w}_{\text{cluster}}) + \sum_{h=1}^H \frac{N_h \|\mathbf{W}_h - \mathbf{W}(\mathcal{K})\|_2^2}{mN}, \quad (9)$$

where  $\mathcal{K}$  denotes the set of all the clients. We have  $\mathbb{V}(\mathbf{w}_{\text{cluster}}) < \mathbb{V}(\mathbf{w}_{\text{rand}})$ , unless  $\forall h \in \{1, \dots, H\}$ ,  $\mathbf{W}_h = \mathbf{W}(\mathcal{K})$ , i.e., each cluster has the same averaged model update with the entire population, which indicates that all the clusters are homogeneous in terms of the mean model update.

**Comparison of Plain Clustering and Clustering with Re-allocation.** We derive the Equation 10 to show the relationship between  $\mathbb{V}(\mathbf{w}_{\text{cldiv}})$  and  $\mathbb{V}(\mathbf{w}_{\text{cluster}})$ :

$$\mathbb{V}(\mathbf{w}_{\text{cluster}}) = \mathbb{V}(\mathbf{w}_{\text{cldiv}}) + \sum_{h=1}^H \frac{N_h (S_h - S)^2}{mN}. \quad (10)$$

We have  $\mathbb{V}(\mathbf{w}_{\text{cldiv}}) < \mathbb{V}(\mathbf{w}_{\text{cluster}})$ , unless  $\forall h \in \{1, \dots, H\}$ ,  $S_h = S$ , i.e., each cluster has equal variability, which indicates that all the clusters are homogeneous in terms of the variability.

**Comparison of Clustering with Re-allocation and HCSFed.** We derive the Equation 11 to show the relationship between  $\mathbb{V}(\mathbf{w}_{\text{cldiv}})$  and  $\mathbb{V}(\mathbf{w}_{\text{hybrid}})$ :

$$\mathbb{V}(\mathbf{w}_{\text{cldiv}}) = \mathbb{V}(\mathbf{w}_{\text{hybrid}}) + \frac{\left(\sum_{i=1}^{N_h} \|G_i\|_2\right)^2}{N_h} \sum_{i=1}^{N_h} \left(I_i - \frac{1}{N_h}\right)^2. \quad (11)$$

We have  $\mathbb{V}(\mathbf{w}_{\text{hybrid}}) < \mathbb{V}(\mathbf{w}_{\text{cldiv}})$ , unless  $\forall i \in \{1, \dots, N_h\}$ ,  $I_i = \frac{\|G_i\|_2}{\sum_{i=1}^{N_h} \|G_i\|_2} = \frac{1}{N_h}$ , i.e., each client in  $h^{\text{th}}$  cluster has equal norm of model update.

**Remark.** *Theorem 1 verifies the capability of HCSFed in variance reduction. The proof sketch indicates that the variance difference of different selections will vanish only if all the clusters and the norm of the gradients are identical. The proposed approach can achieve variance reduction, since each cluster never has identical update mean, variability, and norm in heterogeneous FL.*

### 4.2 Convergence Behavior of HCSFed

We emphasize that the convergence analysis of FedAvg with random selection is **NOT** our contribution, we just follow the previous analysis work [18] to verify that HCSFed could maintain the same convergence guarantees as a random selection in the worst case and in most cases, HCSFed will have tighter convergence compared with random selection.

We next state the assumptions used in our theorem and proof, which are common in the federated optimization literature, e.g., [30, 18, 26, 24, 8, 7]. Assume each function  $F_k$  ( $k \in [N]$ ) is  $\mu$ -strongly convex and  $L$ -smooth. Suppose that for all  $k \in [N]$  and all  $t$ , the variance and expectation of stochastic gradients in each client on random samples  $\xi$  are bounded by  $\sigma_k^2$  and  $G^2$ , i.e.,

$\mathbb{E} \left[ \|\nabla F_k(\mathbf{w}_t^k, \xi) - \nabla F_k(\mathbf{w}_t^k)\|_2^2 \right] \leq \sigma_k^2$  and  $\mathbb{E} \left[ \|\nabla F_k^2(\mathbf{w}_t^k, \xi)\|_2^2 \right] \leq G^2$ , respectively. And  $\Gamma$  is used to quantify the heterogeneity, where  $\Gamma = F^* - \sum_{k=1}^N p_k F_k^*$ .

**Theorem 2** (Convergence Bound). *Let Assumptions above hold and  $L, \mu, \sigma_k, G$  be defined therein. Consider FedAvg when sampling  $m$  clients, then HCSFed satisfies:*

$$\mathbb{E}[F(\mathbf{w}_T)] - F^* \leq \underbrace{\mathcal{O}\left(\frac{\sum_{k=1}^N p_k^2 \sigma_k^2 + E^2 G^2 + \gamma G^2}{\mu T}\right)}_{\text{Bounding FedAvg with Full Participation}} + \mathcal{O}\left(\frac{L\Gamma}{\mu T}\right) + \underbrace{\mathcal{O}\left(\frac{E^2 G^2}{m\mu T}\right)}_{\text{Bounding Variance}}. \quad (12)$$

**Remark.** *Theorem 2 [18] gives the convergence upper bound of FedAvg with hybrid client selection. The first two terms are used to bound the FedAvg with full client participant, while the last term is used to bound the variance of the model update aggregated from the subset. In Theorem 1, we demonstrate the effectiveness of HCSFed in variance reduction. HCSFed achieves a lower variance, which indicates that HCSFed could enjoy a tighter convergence bound.*

**Remark.** *Theorem 2 [18] uses Lemma 1-3 to bound the error of FedAvg with full participation corresponding to the first two terms, while using Lemma 4 to verify the unbiased property and Lemma 5 to bound the variance resulting from the client selection. Theorem 1 shows the effectiveness of HCSFed to reduce selection variance, which also indicates that the variance of HCSFed is always lower than the mentioned selections unless the population is homogeneous. Naturally, HCSFed satisfies the Lemma 5. The dependency between the Lemmas and Theorem 2 indicates that the proof the Lemma 4 is enough to maintain the convergence bound. We defer the proof to Appendix A.3.*

We demonstrate the convergence guarantee of HCSFed under  $\mu$ -strongly convex assumption. As for the non-convex loss function, we refer to the previous proved proposition that FedAvg with any unbiased selections maintains the same FL convergence bound of random selection (Theorem 2 in [6]).

## 5 Experiment

### 5.1 Experimental Setup

We run logistic regression (convex) and a fully connected network with one hidden layer of 50 nodes (non-convex) on MNIST [16]. As for CIFAR-10 [15] and FMNIST [27], we use the same classifier of FedAvg [19] composed of 3 convolutional and 2 fully connected layers. We partition the dataset into 100 clients under both IID and non-IID data distribution. IID data partition strategy employs the idea of random split to create a uniform federated dataset. As for non-IID data partition, we use Dirichlet distribution to partition the entire client set. Dirichlet distribution, i.e.,  $\text{Dir}(\alpha)$ , gives to each client the respective partitioning across labels by changing the value of  $\alpha$ . Specifically, the lower the value of  $\alpha$ , the more heterogeneous the dataset is. The schematic table of the Dirichlet distribution is presented in Appendix A.1. As for the hyperparameters,  $N$  is the number of all clients,  $q$  is the sampling ratio,  $nSGD$  is the times of SGD running locally,  $\eta$  is the learning rate,  $B$  is the batch size,  $T$  is the terminate round. For better comparison, we set all the hyperparameters following the popular FL optimization work FedProx [17].

### 5.2 Main Results

Our evaluation target is to compare the convergence speed of different methods in convex and non-convex FL context. We choose image classification as our downstream task and compare HCSFed with simple random sampling [19], norm-based importance sampling [3], cluster sampling [6], and SCAFFOLD [11]. For better representation of the convergence speed, we follow the previous FL acceleration work setting [11] and report the required rounds for different methods with convex model to reach the target test accuracy in Table 1. We can observe that HCSFed consistently achieves the fastest convergence (has the fewest required rounds to reach the target accuracy) across all settings, surpassing not only the client selection schemes but also the SOTA variance-reduced method SCAFFOLD [11]. We also run HCSFed with non-convex model on different datasets. The result of non-convex experiment is presented in Figure 3. HCSFed consistently requires the fewest rounds to reach the target accuracy. All the results reveal that HCSFed can greatly accelerate the convergence,

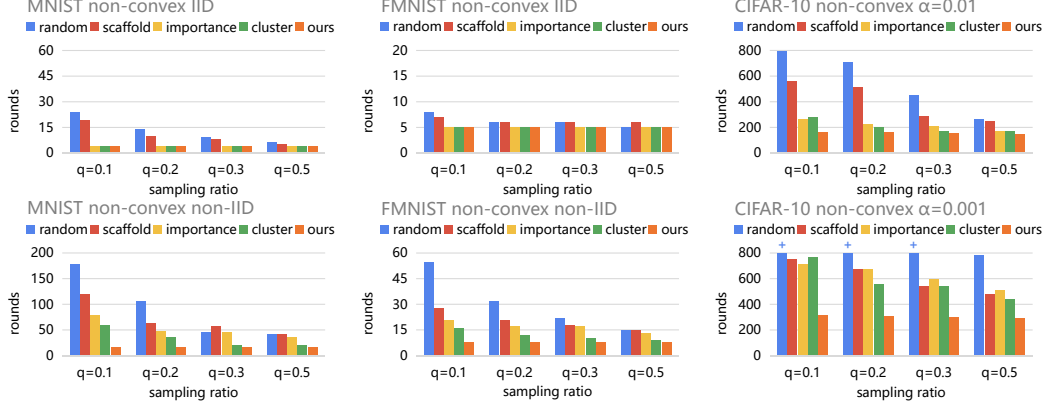


Figure 3: Required rounds for random, cluster, importance sampling, SCAFFOLD, and HCSFed to achieve 60% accuracy with  $q = 0.1$ ,  $N = 100$ ,  $nSGD = 50$ ,  $\eta = 0.01$ ,  $B = 50$  on MNIST and FMNIST, with  $\alpha \in \{0.01, 0.001\}$ ,  $q = 0.1$ ,  $N = 100$ ,  $nSGD = 80$ ,  $\eta = 0.05$ ,  $B = 50$  on CIFAR-10.

especially in the low sampling ratio and data heterogeneity case. As we emphasized in the theoretical analysis, the improvement of HCSFed depends on the sampling ratio and the client heterogeneity. The lower the sampling ratio and the more heterogeneous the dataset, the more improvement HCSFed can enjoy. Naturally, such great improvement in convergence speed can be attributed to the two key components in HCSFed: (i) Different from the previous raw gradient-based methods, we introduce gradient compression to improve the clustering effect by using the more expressive cluster feature representation. (ii) To further guarantee the robustness of the sampling effect, we introduce a sample size re-allocation scheme and extra importance sampling to control the sampling effect fluctuation in the cluster with low client similarity. For more details, please refer to Appendix C.

### 5.3 Parameter Sensitivity Study

**The Number of Clusters (H).** This experiment demonstrates the sensitivity of HCSFed to the different numbers of clusters. We run convex model-based HCSFed on non-IID MNIST with different numbers of clusters, i.e. with  $H \in \{5, 6, \dots, 10\}$ . We report the best classification accuracy and the required rounds for HCSFed with different numbers of clusters to reach the best test accuracy in Figure 4(a). HCSFed achieves stable classification accuracy and similar convergence speeds (measured by the required rounds to achieve the best accuracy), which highlights the robust effect and efficiency of HCSFed. The results also reveal that the clustering effect of HCSFed is robust regardless of the number of clusters. Such merit might attribute to the sample size re-allocation scheme or the importance sampling scheme that we use to control the clustering effect fluctuation.

Table 1: Required rounds for different methods with convex model (logistic regression) to achieve 80% accuracy on non-IID MNIST and FMNIST. 200+ indicates 80% accuracy was not reached after 200 rounds.

Methods	Sampling Ratio 10%		Sampling Ratio 30%		Sampling Ratio 50%		
	Num. of Rounds	Speedup	Num. of Rounds	Speedup	Num. of Rounds	Speedup	
MNIST	Random	96	(1.0x)	42	(1.0x)	28	(1.0x)
	SCAFFOLD	74	(1.3x)	36	(1.2x)	21	(1.3x)
	Importance	35	(2.7x)	24	(1.8x)	22	(1.3x)
	Cluster	31	(3.1x)	16	(2.6x)	8	(3.5x)
	<b>HCSFed</b>	<b>9</b>	<b>(10.7x)</b>	<b>8</b>	<b>(5.2x)</b>	<b>8</b>	<b>(3.5x)</b>
FMNIST	Random	200+	(1.0x)	200+	(1.0x)	158	(1.0x)
	SCAFFOLD	180	(>1.1x)	144	(>1.4x)	115	(1.4x)
	Importance	180	(>1.1x)	116	(>1.7x)	100	(1.6x)
	Cluster	145	(>1.4x)	104	(>1.9x)	75	(2.1x)
	<b>HCSFed</b>	<b>81</b>	<b>(&gt;2.5x)</b>	<b>80</b>	<b>(&gt;2.5x)</b>	<b>75</b>	<b>(2.1x)</b>

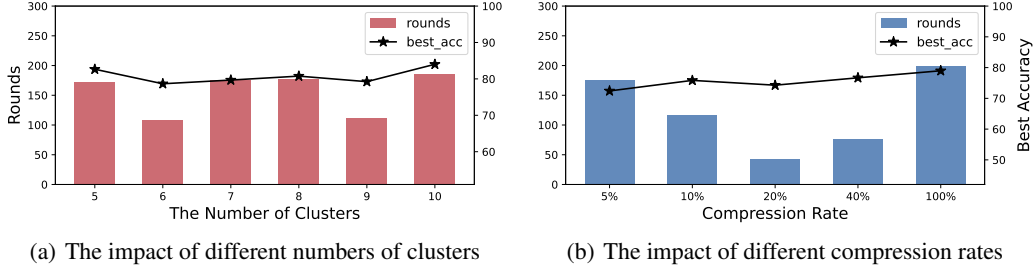


Figure 4: Visualization of Sensitivity Study Results on non-IID MNIST.

**The Compression Rate (R).** We also evaluate how different compression rates affect the global model performance. We run convex model-based  $\text{HCSFed}$  on non-IID MNIST with different compression rates (R), i.e. with  $R \in \{5\%, 10\%, 20\%, 40\%, 100\%\}$ . We report the best accuracy and the required rounds of  $\text{HCSFed}$  with different compression rates to reach the best test accuracy in Figure 4(b). The results show that  $\text{HCSFed}$  achieves different convergence speed as the compression rate changes. The noticeable information is that both too high and too low compression rates can not achieve good learning efficiency. Intuitively, the low compression rate can not ensure the integrity of gradient information while the high compression rate is too complicated to learn efficiently. When we set the compressed rate to 100%, i.e., without gradient compression, the results show that both the convergence speed and final accuracy of the model are not satisfactory, which confirms the effectiveness of gradient compression. In practice, following the previous compression work [9], we set the compression rate with the highest within-group sum of squares to get a good sampling effect.

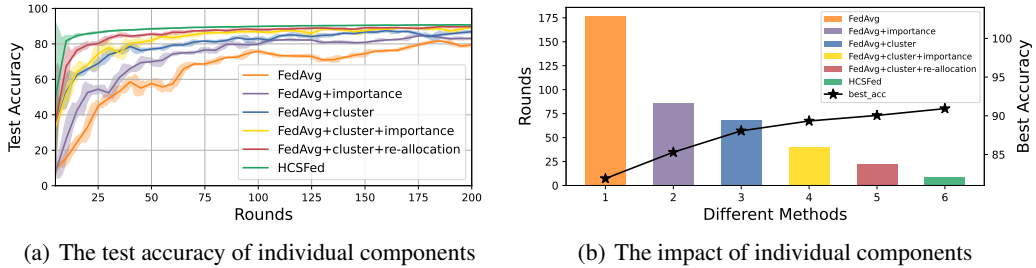


Figure 5: Visualization of Ablation Study Results on non-IID MNIST.

## 5.4 Ablation Study

We run logistic regression (convex) on non-IID MNIST with  $q = 0.1$ ,  $nSGD = 50$  to analyse the individual contributions of different components of  $\text{HCSFed}$  in both final accuracy and convergence speed. In Figure 5(a),  $\text{HCSFed}$  is represented as the green line starting from the accuracy of 10% and ending at 91%, whereas  $\text{FedAvg}$  is the yellow line starting also from the same position as  $\text{HCSFed}$  but ending at 81% after 200 rounds, i.e., 10% less. We report the required rounds for different methods to achieve 80% accuracy in Figure 5(b). Compared with the plain  $\text{FedAvg}$ ,  $\text{FedAvg}$  combined with cluster (blue) or importance sampling (purple) can accelerate the convergence speed (measured by the required rounds to achieve the target accuracy) by  $2.6\times$  and  $2.1\times$  times. The experimental results confirm the important role of the two in improving the learning efficiency. Impressively, compared with importance sampling, the improvement of the clustering process is more obvious. This is because clustering can make better use of the correlation among clients, thereby selecting more representative clients to participate in model training. We also compare  $\text{FedAvg}$  combined with cluster,  $\text{FedAvg}$  combined with cluster and re-allocation,  $\text{FedAvg}$  combined with cluster and importance sampling, and  $\text{HCSFed}$ . All the latter methods can achieve a faster convergence in model training than the former, which validates the effectiveness of re-allocation and extra importance sampling. These results indicate that each component of  $\text{HCSFed}$  is complementary to each other, and also show the effectiveness of the variance reduction theory in Section 4.

## 6 Concluding Remarks

In this paper, we propose  $\text{HCSFed}$ , a novel hybrid clustering-based selection scheme to accelerate the training convergence by variance reduction. As we mentioned in Section 3.1, the reduced variance leads to faster convergence. Therefore,  $\text{HCSFed}$  can achieve communication cost reduction, as it requires fewer rounds to approach the target training accuracy. Theoretically, we demonstrate the improvement of the proposed scheme in variance reduction. We present the convergence guarantee of our proposed approach under the convex assumption. Experimental results demonstrate the superiority and the effectiveness of our method with both the convex and non-convex models. In the future, the co-variance among different clients and unavailable client settings will be considered, since it may also lead to performance degradation in FL. In the theoretical aspect, following the latest convergence analysis [13], we plan to loose the widely used but strict assumption “bounded gradient” and convexity for more general analysis of the faster convergence achieved by  $\text{HCSFed}$ .

## References

- [1] Ravikumar Balakrishnan, Tian Li, Tianyi Zhou, Nageen Himayat, Virginia Smith, and Jeff Bilmes. Diverse client selection for federated learning via submodular maximization. In *International Conference on Learning Representations*, 2022.
- [2] Tianyi Chen, Georgios Giannakis, Tao Sun, and Wotao Yin. Lag: Lazily aggregated gradient for communication-efficient distributed learning. *Advances in Neural Information Processing Systems*, 2018.
- [3] Wenlin Chen, Samuel Horvath, and Peter Richtarik. Optimal client sampling for federated learning. *arXiv preprint arXiv:2010.13723*, 2020.
- [4] Yae Jee Cho, Jianyu Wang, and Gauri Joshi. Client selection in federated learning: Convergence analysis and power-of-choice selection strategies. *arXiv preprint arXiv:2010.01243*, 2020.
- [5] Aymeric Dieuleveut, Gersende Fort, Eric Moulines, and Geneviève Robin. Federated expectation maximization with heterogeneity mitigation and variance reduction. *arXiv preprint arXiv:2111.02083*, 2021.
- [6] Yann Fraboni, Richard Vidal, Laetitia Kameni, and Marco Lorenzi. Clustered sampling: Low-variance and improved representativity for clients selection in federated learning. In *International Conference on Machine Learning*, 2021.
- [7] Farzin Haddadpour, Mohammad Mahdi Kamani, Mehrdad Mahdavi, and Viveck Cadambe. Local sgd with periodic averaging: Tighter analysis and adaptive synchronization. *Advances in Neural Information Processing Systems*, 2019.
- [8] Farzin Haddadpour and Mehrdad Mahdavi. On the convergence of local descent methods in federated learning. *arXiv preprint arXiv:1910.14425*, 2019.
- [9] Song Han, Huizi Mao, and William J Dally. Deep compression: Compressing deep neural networks with pruning, trained quantization and huffman coding. *arXiv preprint arXiv:1510.00149*, 2015.
- [10] Peter Kairouz, H Brendan McMahan, Brendan Avent, Aurélien Bellet, Mehdi Bennis, Arjun Nitin Bhagoji, Kallista Bonawitz, Zachary Charles, Graham Cormode, Rachel Cummings, et al. Advances and open problems in federated learning. *Foundations and Trends® in Machine Learning*, 14(1–2):1–210, 2021.
- [11] Sai Praneeth Karimireddy, Satyen Kale, Mehryar Mohri, Sashank Reddi, Sebastian Stich, and Ananda Theertha Suresh. Scaffold: Stochastic controlled averaging for federated learning. In *International Conference on Machine Learning*, 2020.
- [12] Angelos Katharopoulos and François Fleuret. Not all samples are created equal: Deep learning with importance sampling. In *International Conference on Machine Learning*, 2018.
- [13] Ahmed Khaled, Konstantin Mishchenko, and Peter Richtárik. Tighter theory for local sgd on identical and heterogeneous data. In *International Conference on Artificial Intelligence and Statistics*, 2020.
- [14] Jakub Konečný, Brendan McMahan, and Daniel Ramage. Federated optimization: Distributed optimization beyond the datacenter. *arXiv preprint arXiv:1511.03575*, 2015.
- [15] Alex Krizhevsky, Geoffrey Hinton, et al. Learning multiple layers of features from tiny images. 2009.
- [16] Yann LeCun. The mnist database of handwritten digits. <http://yann.lecun.com/exdb/mnist/>, 1998.
- [17] Tian Li, Anit Kumar Sahu, Manzil Zaheer, Maziar Sanjabi, Ameet Talwalkar, and Virginia Smith. Federated optimization in heterogeneous networks. *Proceedings of Machine Learning and Systems*, 2020.
- [18] Xiang Li, Kaixuan Huang, Wenhao Yang, Shusen Wang, and Zhihua Zhang. On the convergence of fedavg on non-iid data. In *International Conference on Learning Representations*, 2019.
- [19] Brendan McMahan, Eider Moore, Daniel Ramage, Seth Hampson, and Blaise Aguera y Arcas. Communication-efficient learning of deep networks from decentralized data. In *International Conference on Artificial Intelligence and Statistics*, 2017.

- [20] Ihab Mohammed, Shadha Tabatabai, Ala Al-Fuqaha, Faissal El Bouanani, Junaid Qadir, Basheer Qolomany, and Mohsen Guizani. Budgeted online selection of candidate iot clients to participate in federated learning. *IEEE Internet of Things Journal*, 2020.
- [21] Khalil Muhammad, Qinqin Wang, Diarmuid O’Reilly-Morgan, Elias Tragos, Barry Smyth, Neil Hurley, James Geraci, and Aonghus Lawlor. Fedfast: Going beyond average for faster training of federated recommender systems. In *International Conference on Knowledge Discovery & Data Mining*, 2020.
- [22] Elsa Rizk, Stefan Vlaski, and Ali H Sayed. Optimal importance sampling for federated learning. In *IEEE International Conference on Acoustics, Speech and Signal Processing*, 2021.
- [23] Navjot Singh, Deepesh Data, Jemin George, and Suhas Diggavi. Sparq-sgd: Event-triggered and compressed communication in decentralized stochastic optimization. *arXiv preprint arXiv:1910.14280*, 2019.
- [24] Sebastian U Stich. Local sgd converges fast and communicates little. In *International Conference on Learning Representations*, 2018.
- [25] Sebastian U Stich, Jean-Baptiste Cordonnier, and Martin Jaggi. Sparsified sgd with memory. *Advances in Neural Information Processing Systems*, 2018.
- [26] Jianyu Wang and Gauri Joshi. Cooperative sgd: A unified framework for the design and analysis of local-update sgd algorithms. *Journal of Machine Learning Research*, 22:1–50, 2021.
- [27] Han Xiao, Kashif Rasul, and Roland Vollgraf. Fashion-mnist: a novel image dataset for benchmarking machine learning algorithms. *arXiv preprint arXiv:1708.07747*, 2017.
- [28] Yuchen Zhang, John C Duchi, and Martin J Wainwright. Communication-efficient algorithms for statistical optimization. *The Journal of Machine Learning Research*, pages 3321–3363, 2013.
- [29] Peilin Zhao and Tong Zhang. Stochastic optimization with importance sampling for regularized loss minimization. In *International Conference on Machine Learning*, 2015.
- [30] Fan Zhou and Guojing Cong. On the convergence properties of a  $k$ -step averaging stochastic gradient descent algorithm for nonconvex optimization. *arXiv preprint arXiv:1708.01012*, 2017.

## A Extra Illustration

### A.1 Dirichlet Distribution Illustration

Given different values of the concentration parameter  $\alpha$  for the Dirichlet distribution, datasets with different degrees of heterogeneity can be generated. In particular, higher values of  $\alpha$  lead to a more uniform distribution, indicating that each client has an almost equally weighted combination of labels. Lower values of  $\alpha$  imply weights concentrated more heavily on only one of the labels, or more extreme label membership. Table 2 is an example of Dirichlet distribution used in the experiments. As shown in the Table 2, the data distribution on each client is different, and in the case of extreme non-IID, i.e.,  $\alpha \rightarrow 0$ , most of the data are concentrated under only one label, while the amount of others is almost zero.

Table 2: The actual Dirichlet Distribution (non-IID) generated from CIFAR-10 with  $\alpha = 0.001$

Client ID	Numbers of Samples in the Classes										Distribution
	$c_0$	$c_1$	$c_2$	$c_3$	$c_4$	$c_5$	$c_6$	$c_7$	$c_8$	$c_9$	
k=0	2	1	33	117	100	6	1	<b>0</b>	1	239	
k=1	<b>0</b>	<b>0</b>	<b>0</b>	1	1	29	<b>467</b>	<b>0</b>	<b>0</b>	2	
k=2	2	<b>397</b>	5	1	2	86	<b>0</b>	1	<b>0</b>	6	
k=3	1	<b>0</b>	<b>0</b>	<b>0</b>	<b>0</b>	3	<b>0</b>	<b>0</b>	125	<b>371</b>	
k=4	1	67	5	<b>0</b>	15	<b>304</b>	<b>0</b>	<b>0</b>	34	74	
...	...	...	...	...	...	...	...	...	...	...	...
k=95	32	213	<b>0</b>	94	17	3	138	<b>0</b>	<b>0</b>	3	
k=96	51	36	166	32	<b>0</b>	<b>0</b>	8	203	<b>0</b>	4	
k=97	25	<b>0</b>	<b>347</b>	17	7	<b>0</b>	<b>0</b>	44	<b>0</b>	60	
k=98	<b>0</b>	1	<b>0</b>	2	1	18	3	60	<b>413</b>	2	
k=99	<b>465</b>	<b>0</b>	4	2	2	3	4	14	4	2	

### A.2 Gradient Compress Algorithm

---

#### Algorithm 3: GC(Gradient Compress)

---

**Input:** Raw updates in the  $t^{th}$  round of the  $k^{th}$  client  $G_t^k = \{g_1, g_2, \dots, g_d\}$

- 1 **Initialize** Randomly select  $d'$   $g_i$  as the group centers  $\{x_1, x_2, \dots, x_{d'}\}$ ;
- 2 **Initialize**  $C_j = \emptyset$  ( $1 \leq j \leq d'$ );
- 3 **repeat**
- 4   **for each**  $g_i, i = 1, 2, \dots, d$  **do**
- 5      $\lambda_i = \arg \min_{j \in \{1, 2, \dots, d'\}} \|g_i - x_j\|_2$ ;
- 6      $C_{\lambda_i} = C_{\lambda_i} \cup \{g_i\}$ ;
- 7   **end**
- 8   **for each cluster**  $j = 1, 2, \dots, d'$  **do**
- 9     Calculate new center  $x'_j = \frac{1}{|C_j|} \sum_{g_i \in C_j} g_i$ ;
- 10     $x_j \leftarrow x'_j$ ;
- 11   **end**
- 12 **until**  $\forall j = \{1, 2, \dots, d'\}, x'_j = x_j$ ;

**Output:**  $X_t^k = \{x_1, x_2, \dots, x_{d'}\}$ ;

---

### A.3 Key Lemmas

Following [18], we present necessary assumptions and extra notations that we used to prove the convergence of FedAvg with random client selection.

**Assumptions.** The convergence of FedAvg with random sampling scheme has been derived in [18]. The proof relies on the assumptions as follows. Assumptions 3 and 4 have been given by [28, 24, 25].

**Assumption 1** (L-Smooth).  $\forall \mathbf{v}$  and  $\mathbf{w}, k = 1, \dots, N, F_k(\mathbf{v}) \leq F_k(\mathbf{w}) + (\mathbf{v} - \mathbf{w})^T \nabla F_k(\mathbf{w}) + \frac{L}{2} \|\mathbf{v} - \mathbf{w}\|_2^2$  where the  $\mathbf{v}, \mathbf{w}$  are different model parameters.

**Assumption 2** (Strongly Convex).  $\forall \mathbf{v}$  and  $\mathbf{w}, k = 1, \dots, N, F_k(\mathbf{v}) \geq F_k(\mathbf{w}) + (\mathbf{v} - \mathbf{w})^T \nabla F_k(\mathbf{w}) + \frac{\mu}{2} \|\mathbf{v} - \mathbf{w}\|_2^2$  where the  $\mathbf{v}, \mathbf{w}$  are different model parameters.

**Assumption 3** (Bounded Variance). Let  $\xi_t^k$  be sampled from the  $k^{\text{th}}$  device's local data uniformly at random. The variance of stochastic gradients in each device is bounded:

$$\mathbb{E} \|\nabla F_k(\mathbf{w}_t^k, \xi_t^k) - \nabla F_k(\mathbf{w}_t^k)\|^2 \leq \sigma_k^2, \forall k = 1, \dots, N$$

**Assumption 4** (Bounded Expectation). The expectation of stochastic gradients in squared norm is bounded by  $G^2$ , i.e.,

$$\mathbb{E} \|\nabla F_k(\mathbf{w}_t^k, \xi_t^k)\|^2 \leq G^2, \forall k = 1, \dots, N, t = 1, \dots, T - 1$$

**Additional Notation** We assume that FedAvg always activates all devices at the beginning of each round and then uses the parameters maintained in only a few sampled devices to produce the next-round parameter. This updating scheme is equivalent to the original. Let  $\mathcal{I}_E$  be the set of global synchronization, i.e.,  $\mathcal{I}_E = \{nE \mid n = 1, 2, \dots\}$ . If  $t + 1 \in \mathcal{I}_E$ , i.e., the time step to communicate. Then the update of FedAvg with partial devices active can be described as: for all  $k \in [N]$ ,

$$\mathbf{v}_{t+1}^k = \mathbf{w}_t^k - \eta_t \nabla F_k(\mathbf{w}_t^k, \xi_t^k) \quad (13)$$

$$\mathbf{w}_{t+1}^k = \begin{cases} \mathbf{v}_{t+1}^k & , \text{if } t + 1 \notin \mathcal{I}_E \\ \text{average } \{\mathbf{v}_{t+1}^k\}_{k \in \mathcal{S}_{t+1}} & , \text{if } t + 1 \in \mathcal{I}_E, \end{cases} \quad (14)$$

where  $\mathcal{S}_{t+1}$  denotes the subset of  $(t + 1)^{\text{th}}$  round. Here, an additional variable  $\mathbf{v}_{t+1}^k$  is introduced to represent the immediate result of one step SGD update from  $\mathbf{w}_t^k$ . We interpret  $\mathbf{w}_{t+1}^k$  as the parameter obtained after communication steps. Let  $F^*$  and  $F_k^*$  be the minimum values of  $F$  and  $F_k$ , respectively. We use the term  $\Gamma = F^* - \sum_{k=1}^N p_k F_k^*$  for quantifying the degree of non-IID, where the  $p_k$  denotes the aggregation weight. If the data are IID, then  $\Gamma$  goes to zero as the number of samples grows. If the data are non-IID, then  $\Gamma$  is nonzero, and its magnitude reflects the heterogeneity of the data distribution.

**Lemma 1** (Results of one step SGD). Assume Assumption 1 and 2. If  $\eta_t \leq \frac{1}{4L}$ , we have

$$\mathbb{E} \|\bar{\mathbf{v}}_{t+1} - \mathbf{w}^*\|^2 \leq (1 - \eta_t \mu) \mathbb{E} \|\bar{\mathbf{w}}_t - \mathbf{w}^*\|^2 + \eta_t^2 \mathbb{E} \|G_t - \bar{G}_t\|^2 + 6L\eta_t^2 \Gamma + 2\mathbb{E} \sum_{k=1}^N p_k \|\bar{\mathbf{w}}_t - \mathbf{w}_t^k\|^2$$

where  $\Gamma = F^* - \sum_{k=1}^N p_k F_k^* \geq 0$ ,

**Lemma 2** (Bounding the variance). Assume Assumption 3 holds, and  $\sigma_k$  defined there. It follows that

$$\mathbb{E} \|G_t - \bar{G}_t\|^2 \leq \sum_{k=1}^N p_k^2 \sigma_k^2,$$

where the  $G_t$  is the gradient vector of  $t^{\text{th}}$  round.

**Lemma 3** (Bounding the divergence of  $\{\mathbf{w}_t^k\}$ ). Assume Assumption 4, that  $\eta_t$  is non-increasing and  $\eta_t \leq 2\eta_{t+E}$  for all  $t \geq 0$ . It follows that

$$\mathbb{E} \left[ \sum_{k=1}^N p_k \|\bar{\mathbf{w}}_t - \mathbf{w}_t^k\|^2 \right] \leq 4\eta_t^2 (E - 1)^2 G^2.$$

**Lemma 4** (Unbiased sampling scheme). *If  $(t + 1)^{th}$  round is the communication round, for our selection with  $\mathcal{S}_t = \{i_1, \dots, i_m\} \subset [N]$  we have*

$$\mathbb{E}[\mathbf{w}(\mathcal{S}_t)] = \mathbf{w}(\mathcal{K}),$$

where  $\mathcal{K}$  denotes the population of clients.

*Proof.*

$$\mathbb{E}[\mathbf{w}(\mathcal{S}_t)] = \mathbb{E}_{\mathcal{S}_t} \sum_{k=1}^m \mathbf{w}_{i_k} = m \mathbb{E}_{\mathcal{S}_t} [\mathbf{w}_{i_1}] = m \sum_{k=1}^N p_k \mathbf{w}_k \quad (15)$$

□

**Lemma 5** (Bounding the variance of  $\mathbf{w}(\mathcal{S}_t)$ ). *For  $t + 1 \in \mathcal{I}_E$ , assume that  $\eta_t$  is non-increasing and  $\eta_t \leq 2\eta_{t+E}$  for all  $t \geq 0$ . We have the following result assuming  $p_1 = p_2 = \dots = p_{m_h} = \frac{1}{N_h}$ , the expected difference between  $\bar{\mathbf{v}}_{t+1}$  and  $\bar{\mathbf{w}}_{t+1}$  is bounded by*

$$\mathbb{E}_{\mathcal{S}_t} \|\bar{\mathbf{v}}_{t+1} - \bar{\mathbf{w}}_{t+1}\|^2 \leq \frac{4}{K} \eta_t^2 E^2 G^2$$

## B Proof of Theorem

### B.1 Proof of Theorem 1 Variance Reduction

**Additional Notation.** Divide the population  $\mathcal{K}$  consisting of  $N$  clients into  $H$  clusters via clustering.

- $N_h$  denotes the number of clients in  $h^{th}$  cluster, s.t.  $\sum_{h=1}^H N_h = N$
- $m_h$  denotes the number of sampled clients from the  $h^{th}$  cluster
- $m$  denotes the sample size, s.t.  $\sum_{h=1}^H m_h = m$
- $\mathbf{w}_{h_i}$  denotes the model update  $\mathbf{w}$  of the  $i^{th}$  client in the  $h^{th}$  cluster
- $\mathbf{w}_h = \sum_{i=1}^{m_h} \frac{\mathbf{w}_{h_i}}{m_h}$  is the sampled averaged model update of the  $h^{th}$  cluster
- $\bar{\mathbf{w}} = \sum_{h=1}^H \frac{m_h \mathbf{w}_h}{m}$  is the overall sampled averaged model update
- $\mathbf{W}_h = \sum_{i=1}^{N_h} \frac{\mathbf{w}_{h_i}}{N_h}$  is the averaged model update of the  $h^{th}$  cluster
- $\mathbf{W}(\mathcal{K}) = \sum_{h=1}^H \sum_{i=1}^{N_h} \frac{\mathbf{w}_{h_i}}{N}$  is the averaged model update of entire set  $\mathcal{K}$
- $\mathbf{w}_{cluster} = \frac{1}{N} \sum_{h=1}^H N_h \mathbf{w}_h$  is an unbiased estimator of  $\mathbf{W}(\mathcal{K})$
- $S^2 = \frac{1}{N} \sum_{i=1}^N \|\mathbf{w}_i - \mathbf{W}(\mathcal{K})\|_2^2 := \frac{1}{N} \sum_{i=1}^N \sigma^2$
- $S_h^2 = \sum_{i=1}^{N_h} \frac{\|\mathbf{w}_{h_i} - \mathbf{W}_h\|_2^2}{N_h - 1}$
- $s_h^2 = \sum_{i=1}^{m_h} \frac{\|\mathbf{w}_{h_i} - \mathbf{w}_h\|_2^2}{m_h - 1}$
- $Q_h = \frac{N_h}{N}$  is the proportion of clients in the  $h^{th}$  cluster
- $q_h = \frac{m_h}{m}$  is the proportion of sampled clients in the  $h^{th}$  cluster

*Proof of Theorem 1. Derive the Variance of Random Selection.* Assuming that each observation has variance  $\sigma^2$ , then we get

$$\mathbb{V}(\mathbf{w}_{rand}) = \mathbb{E} \|\bar{\mathbf{w}} - \mathbf{W}(\mathcal{K})\|_2^2 \quad (16)$$

$$= \frac{1}{m^2} \mathbb{E} \left\| \sum_{i=1}^m [\mathbf{w}_i - \mathbf{W}(\mathcal{K})] \right\|_2^2 \quad (17)$$

$$= \frac{1}{m^2} \mathbb{E} \left[ \sum_{i=1}^m \|\mathbf{w}_i - \mathbf{W}(\mathcal{K})\|_2^2 \right] \quad (18)$$

$$\underbrace{\hspace{10em}}_{\text{Quadratic Term}} + \frac{1}{m^2} \mathbb{E} \left[ \sum_i^m \sum_{j \neq i}^m [\mathbf{w}_i - \mathbf{W}(\mathcal{K})]^T [\mathbf{w}_j - \mathbf{W}(\mathcal{K})] \right] \quad (19)$$

*Cross-Product Term*

$$= \frac{1}{m^2} \sum_{i=1}^m \mathbb{E} \|\mathbf{w}_i - \mathbf{W}(\mathcal{K})\|_2^2 \quad (20)$$

$$+ \frac{1}{m^2} \underbrace{\sum_i^m \sum_{j \neq i}^m \mathbb{E} \left[ [\mathbf{w}_i - \mathbf{W}(\mathcal{K})]^T [\mathbf{w}_j - \mathbf{W}(\mathcal{K})] \right]}_{\text{Setting to } K} \quad (21)$$

$$= \frac{1}{m^2} \sum_{i=1}^m \sigma^2 + \frac{K}{m^2} \quad (22)$$

$$= \frac{N-1}{Nm} S^2 + \frac{K}{m^2}, \quad (23)$$

where we set  $K = \sum_i^m \sum_{j \neq i}^m \mathbb{E} \left[ [\mathbf{w}_i - \mathbf{W}(\mathcal{K})]^T [\mathbf{w}_j - \mathbf{W}(\mathcal{K})] \right]$  for convenience.

**Find the Expression of  $K$ .** In order to find  $K$ , we consider,

$$\mathbb{E} [[\mathbf{w}_i - \mathbf{W}(\mathcal{K})] [\mathbf{w}_j - \mathbf{W}(\mathcal{K})]] = \frac{1}{N(N-1)} \sum_k^N \sum_{\ell \neq k}^N \left[ [\mathbf{w}_k - \mathbf{W}(\mathcal{K})]^T [(\mathbf{w}_\ell - \mathbf{W}(\mathcal{K}))] \right]. \quad (24)$$

Meanwhile, we have,

$$\sum_{k=1}^N [\mathbf{w}_k - \mathbf{W}(\mathcal{K})] = \sum_{k=1}^N \mathbf{w}_k - N\mathbf{W}(\mathcal{K}) \quad (25)$$

$$= N\mathbf{W}(\mathcal{K}) - N\mathbf{W}(\mathcal{K}) = 0, \quad (26)$$

i.e.,

$$\left\| \sum_{k=1}^N [\mathbf{w}_k - \mathbf{W}(\mathcal{K})] \right\|_2^2 = 0. \quad (27)$$

And the left can be constructed as,

$$\left\| \sum_{k=1}^N [\mathbf{w}_k - \mathbf{W}(\mathcal{K})] \right\|_2^2 = \sum_{k=1}^N \|\mathbf{w}_k - \mathbf{W}(\mathcal{K})\|_2^2 \quad (28)$$

$$+ \sum_k^N \sum_{\ell \neq k}^N \left[ [\mathbf{w}_k - \mathbf{W}(\mathcal{K})]^T [\mathbf{w}_\ell - \mathbf{W}(\mathcal{K})] \right]. \quad (29)$$

Simplify it, we will get

$$0 = (N-1)S^2 + \sum_k^N \sum_{\ell \neq k}^N \left[ [\mathbf{w}_k - \mathbf{W}(\mathcal{K})]^T [\mathbf{w}_\ell - \mathbf{W}(\mathcal{K})] \right], \quad (30)$$

equal to,

$$\sum_k^N \sum_{\ell \neq k}^N \left[ [\mathbf{w}_k - \mathbf{W}(\mathcal{K})]^T [\mathbf{w}_\ell - \mathbf{W}(\mathcal{K})] \right] = -(N-1)S^2. \quad (31)$$

Therefore,

$$\frac{1}{N(N-1)} \sum_k^N \sum_{\ell \neq k}^N \left[ [\mathbf{w}_k - \mathbf{W}(\mathcal{K})]^T [\mathbf{w}_\ell - \mathbf{W}(\mathcal{K})] \right] \quad (32)$$

$$= \frac{1}{N(N-1)} [-(N-1)S^2] \quad (33)$$

$$= -\frac{S^2}{N}, \quad (34)$$

thus

$$K = \sum_i^m \sum_{j \neq i}^m \mathbb{E} \left[ [\mathbf{w}_i - \mathbf{W}(\mathcal{K})]^T [\mathbf{w}_j - \mathbf{W}(\mathcal{K})] \right] \quad (35)$$

$$= m(m-1) \frac{1}{N(N-1)} \sum_k^N \sum_{\ell \neq k}^N \left[ [\mathbf{w}_k - \mathbf{W}(\mathcal{K})]^T [\mathbf{w}_\ell - \mathbf{W}(\mathcal{K})] \right] \quad (36)$$

$$= -m(m-1) \frac{S^2}{N}, \quad (37)$$

and substitute the value of  $K$ , the variance of  $\mathbf{w}_{rand}$  is

$$\mathbb{V}(\mathbf{w}_{rand}) = \frac{N-1}{Nm} S^2 - \frac{1}{n^2} m(m-1) \frac{S^2}{N} \quad (38)$$

$$= \frac{N-m}{Nm} S^2. \quad (39)$$

If  $N$  is infinite (large enough), we can get

$$\mathbb{V}(\mathbf{w}_{rand}) = \frac{N-m}{Nm} S^2 \quad (40)$$

$$= \left( \frac{1}{m} - \frac{1}{N} \right) S^2 \cong \frac{S^2}{m}. \quad (41)$$

**Derive the Variance of Plain Clustering Selection.** As prior work constructed, clustering selection is always applied under plain proportional allocation, where the number of sampled clients  $m_h$  from the  $h^{th}$  cluster is proportional to its cluster size  $N_h$ , i.e.,  $m_h = m \frac{N_h}{N}$ . And we have

$$\mathbb{V}(\mathbf{w}_{cluster}) = \sum_{h=1}^H Q_h^2 \mathbb{V}(\mathbf{w}_h) + \sum_{h(\neq j)=1}^H \sum_{j=1}^{m_h} Q_h Q_j \text{Cov}(\mathbf{w}_h, \mathbf{w}_j). \quad (42)$$

For the former we have

$$\mathbb{V}(\mathbf{w}_h) = \frac{N_h - m_h}{N_h m_h} S_h^2, \quad (43)$$

and for the latter (covariance) we have

$$\text{Cov}(\mathbf{w}_h, \mathbf{w}_j) = 0, h \neq j, \quad (44)$$

where

$$S_h^2 = \frac{1}{N_h - 1} \sum_{j=1}^{N_h} \|\mathbf{w}_{h_j} - \mathbf{W}_h\|_2^2, \quad (45)$$

thus

$$\mathbb{V}(\mathbf{w}_{cluster}) = \sum_{h=1}^H \left( \frac{N_h - m_h}{N_h m_h} \right) Q_h^2 S_h^2. \quad (46)$$

Therefore we can get

$$\mathbb{V}(\mathbf{w}_{cluster}) = \sum_{h=1}^H \left( \frac{N_h - \frac{m}{N} N_h}{N_h \frac{m}{N} N_h} \right) \left( \frac{N_h}{N} \right)^2 S_h^2 \quad (47)$$

$$= \frac{N - m}{Nm} \sum_{h=1}^H \frac{N_h S_h^2}{N} \quad (48)$$

$$= \frac{N - m}{Nm} \sum_{h=1}^H Q_h S_h^2 \quad (49)$$

$$\cong \frac{\sum_{h=1}^H N_h S_h^2}{mN}. \quad (50)$$

**Derive the Variance of Clustering Selection with Sample Size Re-allocation.** We apply clustering selection under sample size re-allocation, where the number of sampled clients  $m_h$  from the  $h^{th}$  cluster is proportional to both cluster's size  $N_h$  and the variability of cluster measured by  $S_h$ , i.e.,

$$m_h = \frac{N_h S_h}{\sum_{h=1}^H N_h S_h} \cdot m. \quad (51)$$

We can get

$$\mathbb{V}(\mathbf{w}_{cluidiv}) = \sum_{h=1}^H \left( \frac{1}{m_h} - \frac{1}{N_h} \right) Q_h^2 S_h^2 \quad (52)$$

$$= \sum_{h=1}^H \frac{Q_h^2 S_h^2}{m_h} - \sum_{h=1}^H \frac{Q_h^2 S_h^2}{N_h} \quad (53)$$

$$= \sum_{h=1}^H \left[ Q_h^2 S_h^2 \left( \frac{\sum_{h=1}^H N_h S_h}{mN_h S_h} \right) \right] - \sum_{h=1}^H \frac{Q_h^2 S_h^2}{N_h} \quad (54)$$

$$= \sum_{h=1}^H \left[ \frac{1}{m} \cdot \frac{N_h S_h}{N^2} \left( \sum_{h=1}^H N_h S_h \right) \right] - \sum_{h=1}^H \frac{Q_h^2 S_h^2}{N_h} \quad (55)$$

$$= \frac{1}{m} \left( \sum_{h=1}^H \frac{N_h S_h}{N} \right)^2 - \sum_{h=1}^H \frac{Q_h^2 S_h^2}{N_h} \quad (56)$$

$$= \frac{1}{m} \left( \sum_{h=1}^H Q_h S_h \right)^2 - \frac{1}{N} \sum_{h=1}^H Q_h S_h^2 \quad (57)$$

$$= \frac{1}{N^2} \frac{\left( \sum_{h=1}^H N_h S_h \right)^2}{m} - \frac{1}{N^2} \sum_{h=1}^H N_h S_h^2 \quad (58)$$

$$\cong \frac{1}{mN^2} \left( \sum_{h=1}^H N_h S_h \right)^2. \quad (59)$$

Based on all the above, We have these equations below when approximations are used,

$$\mathbb{V}(\mathbf{w}_{rand}) = \frac{N-m}{Nm} S^2 \quad (60)$$

$$\cong \frac{S^2}{m}, \quad (61)$$

$$\mathbb{V}(\mathbf{w}_{cluster}) = \frac{N-m}{N} \cdot \frac{\sum_{h=1}^H N_h S_h^2}{mN} \quad (62)$$

$$\cong \frac{\sum_{h=1}^H N_h S_h^2}{mN}, \quad (63)$$

$$\mathbb{V}(\mathbf{w}_{cluidiv}) = \frac{1}{N^2} \cdot \frac{\left(\sum_{h=1}^H N_h S_h\right)^2}{m} - \frac{1}{N^2} \sum_{h=1}^H N_h S_h^2 \quad (64)$$

$$\cong \frac{1}{mN^2} \left(\sum_{h=1}^H N_h S_h\right)^2. \quad (65)$$

**Relationship.** In order to compare  $\mathbb{V}(w_{rand})$  and  $\mathbb{V}(w_{cluster})$ , we first attempt to express  $S^2$  as a function of  $S_h^2$ .

$$(N-1)S^2 = \sum_{h=1}^H \sum_{i=1}^{m_h} \|\mathbf{w}_{h_i} - \mathbf{W}(\mathcal{K})\|_2^2 \quad (66)$$

$$= \sum_{h=1}^H \sum_{i=1}^{m_h} \|\mathbf{w}_{h_i} - \mathbf{W}_h\|_2^2 \quad (67)$$

$$+ \sum_{h=1}^H N_h \|\mathbf{W}_h - \mathbf{W}(\mathcal{K})\|_2^2 \quad (68)$$

$$= \sum_{h=1}^H (N_h - 1) S_h^2 + \sum_{h=1}^H N_h \|\mathbf{W}_h - \mathbf{W}(\mathcal{K})\|_2^2 \quad (69)$$

$$\frac{N-1}{N} S^2 = \sum_{h=1}^H \frac{N_h - 1}{N} S_h^2 + \sum_{h=1}^H \frac{N_h}{N} \|\mathbf{W}_h - \mathbf{W}(\mathcal{K})\|_2^2 \quad (70)$$

We assume that  $N_h$  is large enough to permit the approximation for simplification

$$\frac{N_h - 1}{N_h} \approx 1 \text{ and } \frac{N-1}{N} \approx 1 \quad (71)$$

Thus

$$S^2 = \sum_{h=1}^H \frac{N_h}{N} S_h^2 + \sum_{h=1}^H \frac{N_h}{N} \|\mathbf{W}_h - \mathbf{W}(\mathcal{K})\|_2^2 \quad (72)$$

Therefore

$$\mathbb{V}(\mathbf{w}_{rand}) = \frac{S^2}{m} = \frac{\sum_{h=1}^H N_h S_h^2}{mN} \quad (73)$$

$$+ \frac{\sum_{h=1}^H N_h \|\mathbf{W}_h - \mathbf{W}(\mathcal{K})\|_2^2}{mN} \quad (74)$$

$$= \mathbb{V}(\mathbf{w}_{cluster}) + \frac{\sum_{h=1}^H N_h \|\mathbf{W}_h - \mathbf{W}(\mathcal{K})\|_2^2}{mN} \quad (75)$$

which shows that

$$\mathbb{V}(\mathbf{w}_{cluster}) \leq \mathbb{V}(\mathbf{w}_{rand}) \quad (76)$$

Unless  $\mathbf{W}_h = \mathbf{W}(\mathcal{K})$  for every  $h$ , we must have  $\mathbb{V}(\mathbf{w}_{cluidiv}) \leq \mathbb{V}(\mathbf{w}_{cluster})$ . The difference is

$$\mathbb{V}(\mathbf{w}_{cluster}) = \mathbb{V}(\mathbf{w}_{cluidiv}) + \frac{1}{mN} \sum_{h=1}^H N_h (S_h - \bar{S})^2. \quad (77)$$

This shows that

$$\mathbb{V}(\mathbf{w}_{cluidiv}) \leq \mathbb{V}(\mathbf{w}_{cluster}), \quad (78)$$

unless  $S_h = \bar{S}$  for every  $h$ , i.e., the clusters have equal variability. Therefore, we get

$$\mathbb{V}(\mathbf{w}_{cluidiv}) \leq \mathbb{V}(\mathbf{w}_{cluster}) \leq \mathbb{V}(\mathbf{w}_{rand}) \quad (79)$$

In this paper, we proposed to apply the importance selection based on the norm of the gradient to each cluster instead of random selection. Here we present the variance-reduction relationship between random selection and importance selection. Please note that this part is directly adapted from prior importance sampling work [12], which is not our contribution.

$$\text{Tr}(\mathbb{V}_{rand}[G_i]) - \text{Tr}(\mathbb{V}_{import}[c_i G_i]) \quad (80)$$

$$= \mathbb{E}_{rand}[\|G_i\|_2^2] - \mathbb{E}_{import}[c_i^2 \|G_i\|_2^2] \quad (81)$$

Using the fact that  $c_i = \frac{1}{N_h G_i}$ ,  $I_i = \frac{\|G_i\|_2}{\sum_{i=1}^{N_h} \|G_i\|_2}$ ,  $u = \frac{1}{N_h}$ , we have

$$\mathbb{E}_{import}[c_i^2 \|G_i\|_2^2] = \left( \frac{1}{N_h} \sum_{i=1}^{N_h} \|G_i\|_2 \right)^2 \quad (82)$$

Then simplify it, we can get

$$\text{Tr}(\mathbb{V}_{rand}[G_i]) - \text{Tr}(\mathbb{V}_{import}[w_i G_i]) \quad (83)$$

$$= \frac{1}{N_h} \sum_{i=1}^{N_h} \|G_i\|_2^2 - \left( \frac{1}{N_h} \sum_{i=1}^{N_h} \|G_i\|_2 \right)^2 \quad (84)$$

$$= \frac{\left( \sum_{i=1}^{N_h} \|G_i\|_2 \right)^2}{N_h^3} \sum_{i=1}^{N_h} \left( N_h^2 \frac{\|G_i\|_2^2}{\left( \sum_{i=1}^{N_h} \|G_i\|_2 \right)^2} - 1 \right) \quad (85)$$

$$= \frac{\left( \sum_{i=1}^{N_h} \|G_i\|_2 \right)^2}{N_h} \sum_{i=1}^{N_h} (I_i^2 - u^2) \quad (86)$$

Using the fact that  $\sum_{i=1}^{N_h} u = 1$ , we can complete the derivation.

$$\text{Tr}(\mathbb{V}_{rand}[G_i]) - \text{Tr}(\mathbb{V}_{import}[w_i G_i]) \quad (87)$$

$$= \frac{\left( \sum_{i=1}^{N_h} \|G_i\|_2 \right)^2}{N_h} \sum_{i=1}^{N_h} (I_i - u)^2 \quad (88)$$

$$= \left( \frac{1}{N_h} \sum_{i=1}^{N_h} \|G_i\|_2 \right)^2 N_h \|I - u\|_2^2 \quad (89)$$

□

## C Additional Experiments

### C.1 Influence of the Sampling Ratio

As the sampling ratio  $q$  decreases, the performance of all schemes becomes unacceptable except ours.

Table 3: Final test accuracy of multiple FL algorithms with different sampling schemes under convex model on MNIST, FMNIST, setting parameters  $q \in \{0.1, 0.2, 0.3, 0.5\}$ ,  $N = 100$ ,  $nSGD = 50$ ,  $\eta = 0.05$ ,  $B = 50$ .

Methods		MNIST		FMNIST	
		IID	non-IID	IID	non-IID
q=0.1	Random	86.8 $\pm$ 0.0	79.3 $\pm$ 0.6	75.9 $\pm$ 0.0	62.6 $\pm$ 1.0
	SCAFFOLD	84.2 $\pm$ 0.2	78.8 $\pm$ 1.3	73.5 $\pm$ 0.0	70.7 $\pm$ 0.0
	Importance	90.9 $\pm$ 0.0	87.2 $\pm$ 1.2	82.5 $\pm$ 0.1	73.2 $\pm$ 1.6
	Cluster	90.91 $\pm$ 0.0	88.0 $\pm$ 0.4	82.6 $\pm$ 0.1	74.3 $\pm$ 2.0
	<b>HCSFed</b>	90.9 $\pm$ 0.0	<b>89.0 <math>\pm</math>0.0</b>	82.5 $\pm$ 0.1	<b>78.8 <math>\pm</math>0.0</b>
q=0.2	Random	88.4 $\pm$ 0.0	83.2 $\pm$ 0.3	78.6 $\pm$ 0.1	71.6 $\pm$ 1.1
	SCAFFOLD	85.2 $\pm$ 0.0	86.6 $\pm$ 0.2	74.2 $\pm$ 0.0	71.0 $\pm$ 0.0
	Importance	90.8 $\pm$ 0.0	87.5 $\pm$ 1.0	82.6 $\pm$ 0.1	75.1 $\pm$ 2.0
	Cluster	90.89 $\pm$ 0.0	88.6 $\pm$ 0.3	82.5 $\pm$ 0.1	77.3 $\pm$ 1.1
	<b>HCSFed</b>	91.0 $\pm$ 0.0	<b>89.1 <math>\pm</math>0.1</b>	<b>82.5 <math>\pm</math>0.1</b>	<b>78.9 <math>\pm</math>0.1</b>
q=0.3	Random	89.3 $\pm$ 0.0	86.1 $\pm$ 0.2	80.1 $\pm$ 0.1	71.3 $\pm$ 0.2
	SCAFFOLD	84.9 $\pm$ 0.1	87.0 $\pm$ 0.1	74.4 $\pm$ 0.0	71.1 $\pm$ 0.0
	Importance	90.8 $\pm$ 0.0	88.4 $\pm$ 0.4	82.6 $\pm$ 0.0	75.4 $\pm$ 1.9
	Cluster	90.85 $\pm$ 0.0	89.1 $\pm$ 0.1	82.5 $\pm$ 0.0	77.4 $\pm$ 0.5
	<b>HCSFed</b>	90.9 $\pm$ 0.0	<b>89.0 <math>\pm</math>0.0</b>	82.6 $\pm$ 0.1	<b>78.9 <math>\pm</math>0.0</b>
q=0.5	Random	90.0 $\pm$ 0.0	87.2 $\pm$ 0.1	81.2 $\pm$ 0.0	75.5 $\pm$ 0.3
	SCAFFOLD	85.0 $\pm$ 0.1	87.2 $\pm$ 0.1	74.5 $\pm$ 0.0	70.9 $\pm$ 0.0
	Importance	90.9 $\pm$ 0.0	89.0 $\pm$ 0.2	82.5 $\pm$ 0.0	77.2 $\pm$ 1.0
	Cluster	90.87 $\pm$ 0.0	89.0 $\pm$ 0.1	82.5 $\pm$ 0.0	78.7 $\pm$ 0.4
	<b>HCSFed</b>	90.9 $\pm$ 0.0	<b>89.0 <math>\pm</math>0.0</b>	82.5 $\pm$ 0.0	<b>78.9 <math>\pm</math>0.0</b>

Table 4: Final test accuracy of multiple FL algorithms with different sampling schemes under non-convex model on MNIST, FMNIST and CIFAR-10, setting parameters  $q \in \{0.1, 0.2, 0.3, 0.5\}$ ,  $N = 100$ ,  $nSGD = 50$  for MNIST and FMNIST,  $nSGD = 80$  for CIFAR-10,  $\eta = 0.05$ ,  $B = 50$ .

Methods		MNIST		FMNIST		CIFAR-10		
		IID	non-IID	IID	non-IID	IID	$\alpha = 0.01$	$\alpha = 0.001$
q=0.1	Random	87.0 $\pm$ 0.0	59.7 $\pm$ 1.4	87.6 $\pm$ 0.1	76.9 $\pm$ 0.2	40.3 $\pm$ 0.2	25.8 $\pm$ 0.4	20.5 $\pm$ 0.5
	Importance	92.9 $\pm$ 0.1	71.2 $\pm$ 9.5	90.4 $\pm$ 0.1	85.1 $\pm$ 2.2	66.0 $\pm$ 0.2	39.5 $\pm$ 3.3	24.9 $\pm$ 2.6
	Cluster	92.9 $\pm$ 0.0	73.6 $\pm$ 3.7	90.6 $\pm$ 0.2	88.9 $\pm$ 4.6	65.5 $\pm$ 0.3	37.2 $\pm$ 3.9	30.0 $\pm$ 4.7
	<b>HCSFed</b>	92.9 $\pm$ 0.0	<b>83.3 <math>\pm</math>0.0</b>	90.5 $\pm$ 0.1	<b>92.0 <math>\pm</math>0.2</b>	65.7 $\pm$ 0.3	<b>41.2 <math>\pm</math>1.8</b>	<b>38.8 <math>\pm</math>0.6</b>
q=0.2	Random	89.3 $\pm$ 0.0	70.8 $\pm$ 1.6	88.8 $\pm$ 0.0	80.5 $\pm$ 0.5	49.8 $\pm$ 0.4	29.7 $\pm$ 0.3	25.1 $\pm$ 0.2
	Importance	92.9 $\pm$ 0.0	72.9 $\pm$ 9.0	90.3 $\pm$ 0.0	90.8 $\pm$ 0.6	65.7 $\pm$ 0.2	40.7 $\pm$ 2.9	30.5 $\pm$ 2.0
	Cluster	92.9 $\pm$ 0.0	80.3 $\pm$ 1.7	90.4 $\pm$ 0.1	90.7 $\pm$ 1.0	65.6 $\pm$ 0.3	42.0 $\pm$ 1.4	33.0 $\pm$ 3.6
	<b>HCSFed</b>	92.8 $\pm$ 0.0	<b>83.5 <math>\pm</math>0.1</b>	90.4 $\pm$ 0.1	<b>92.1 <math>\pm</math>0.2</b>	65.4 $\pm$ 0.3	<b>41.6 <math>\pm</math>0.9</b>	<b>39.2 <math>\pm</math>2.0</b>
q=0.3	Random	90.1 $\pm$ 0.0	73.4 $\pm$ 2.1	89.4 $\pm$ 0.0	83.7 $\pm$ 0.3	54.8 $\pm$ 0.4	34.9 $\pm$ 0.6	26.6 $\pm$ 0.5
	Importance	92.9 $\pm$ 0.0	76.3 $\pm$ 3.5	90.6 $\pm$ 0.1	90.5 $\pm$ 1.3	65.7 $\pm$ 0.2	42.0 $\pm$ 2.3	32.6 $\pm$ 3.4
	Cluster	92.9 $\pm$ 0.0	81.8 $\pm$ 1.5	90.5 $\pm$ 0.1	91.6 $\pm$ 0.5	66.1 $\pm$ 0.3	43.0 $\pm$ 1.0	34.6 $\pm$ 2.1
	<b>HCSFed</b>	92.8 $\pm$ 0.0	<b>83.3 <math>\pm</math>0.1</b>	90.2 $\pm$ 0.1	<b>92.2 <math>\pm</math>0.1</b>	65.4 $\pm$ 0.3	<b>42.3 <math>\pm</math>0.6</b>	<b>39.7 <math>\pm</math>0.7</b>
q=0.5	Random	91.4 $\pm$ 0.0	80.9 $\pm$ 1.3	90.1 $\pm$ 0.1	87.9 $\pm$ 0.3	61.1 $\pm$ 0.2	39.4 $\pm$ 0.4	30.5 $\pm$ 0.6
	Importance	92.9 $\pm$ 0.0	80.8 $\pm$ 3.8	90.6 $\pm$ 0.1	90.5 $\pm$ 1.5	65.8 $\pm$ 0.3	43.2 $\pm$ 1.2	35.4 $\pm$ 1.7
	Cluster	92.9 $\pm$ 0.0	83.5 $\pm$ 0.2	90.4 $\pm$ 0.1	92.0 $\pm$ 0.2	65.9 $\pm$ 0.4	44.0 $\pm$ 0.6	36.3 $\pm$ 1.0
	<b>HCSFed</b>	92.9 $\pm$ 0.0	<b>83.3 <math>\pm</math>0.1</b>	90.4 $\pm$ 0.1	<b>92.0 <math>\pm</math>0.2</b>	65.7 $\pm$ 0.5	<b>42.4 <math>\pm</math>0.7</b>	<b>39.8 <math>\pm</math>0.6</b>

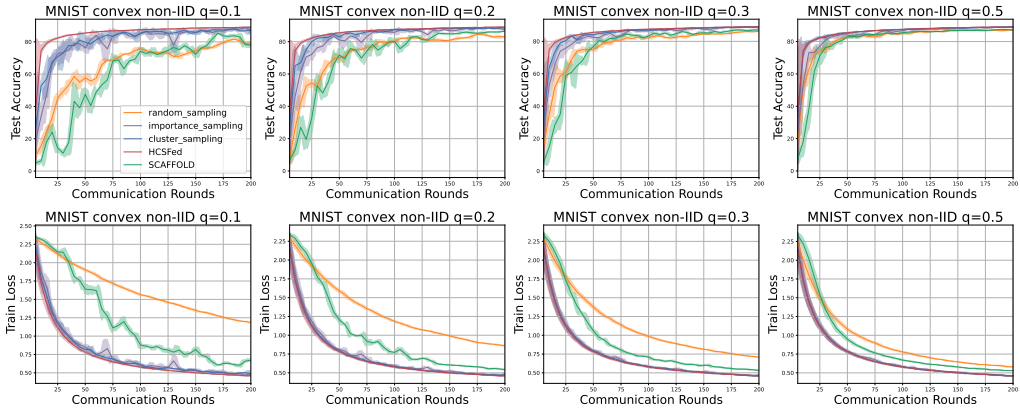


Figure 6: Impact of sampling ratio  $q$  on the performance with convex model. We compare HCSFed with simple random sampling, importance sampling, cluster sampling, SCAFFOLD on MNIST under non-IID, setting parameters  $q \in \{0.1, 0.2, 0.3, 0.5\}$ ,  $N = 100$ ,  $nSGD = 50$ ,  $\eta = 0.01$ ,  $B = 50$ .

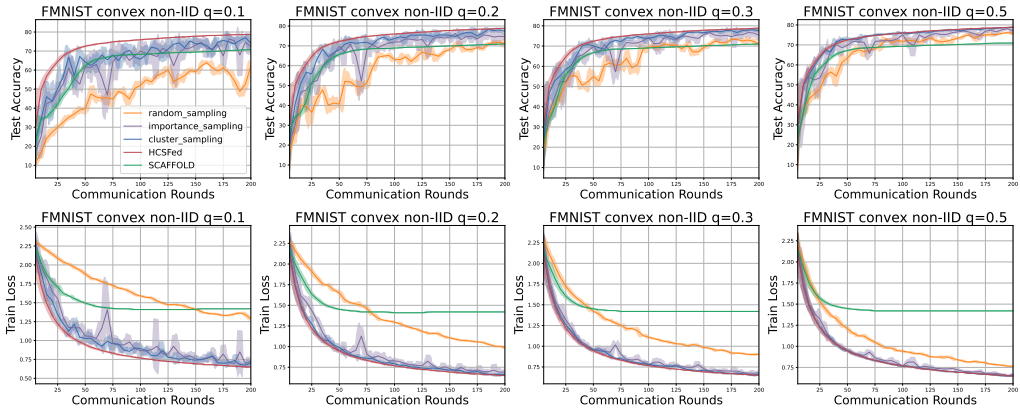


Figure 7: Impact of sampling ratio  $q$  on the performance with convex model. We compare HCSFed with simple random sampling, importance sampling, cluster sampling, SCAFFOLD on FMNIST under non-IID, setting parameters  $q \in \{0.1, 0.2, 0.3, 0.5\}$ ,  $N = 100$ ,  $nSGD = 50$ ,  $\eta = 0.01$ ,  $B = 50$ .

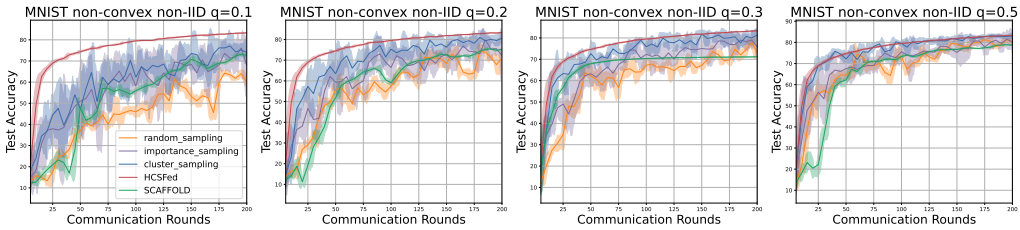


Figure 8: Impact of sampling ratio  $q$  on the performance with non-convex model. We compare HCSFed with simple random sampling, importance sampling, cluster sampling, SCAFFOLD on MNIST under non-IID, setting parameters  $q \in \{0.1, 0.2, 0.3, 0.5\}$ ,  $N = 100$ ,  $nSGD = 50$ ,  $\eta = 0.01$ ,  $B = 50$ .

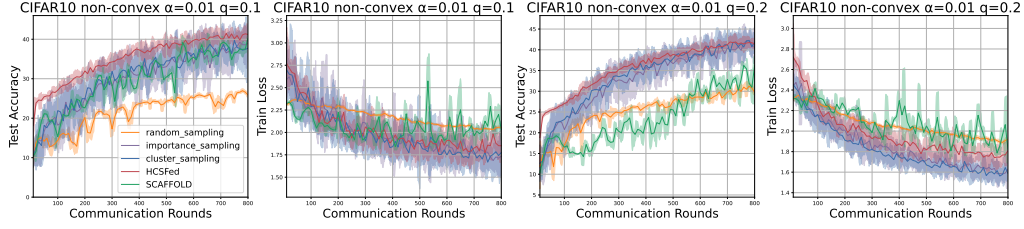


Figure 9: Impact of sampling ratio  $q$  on the performance with non-convex model. We compare  $\text{HCSFed}$  with simple random sampling, importance sampling, cluster sampling, SCAFFOLD on CIFAR-10, using a Dirichlet Distribution with  $\alpha = 0.01$ , setting parameters  $q \in \{0.1, 0.2\}$ ,  $N = 100$ ,  $nSGD = 80$ ,  $\eta = 0.05$ ,  $B = 50$ .

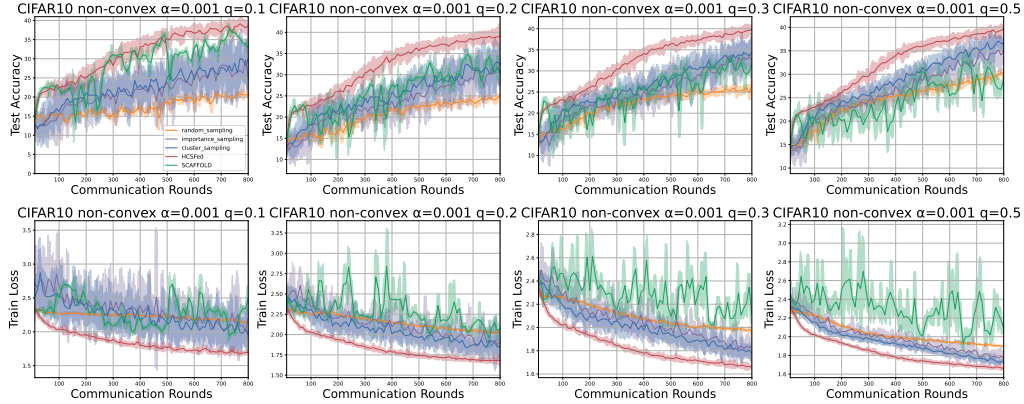


Figure 10: Impact of the heterogeneity on the performance with non-convex model. We compare  $\text{HCSFed}$  with simple random sampling, importance sampling, cluster sampling and SCAFFOLD on CIFAR-10, using a Dirichlet Distribution with  $\alpha = 0.001$ , setting parameters  $q \in \{0.1, 0.2, 0.3, 0.5\}$ ,  $N = 100$ ,  $nSGD = 80$ ,  $\eta = 0.05$ ,  $B = 50$ .

## C.2 Extra Experiments on FedNova

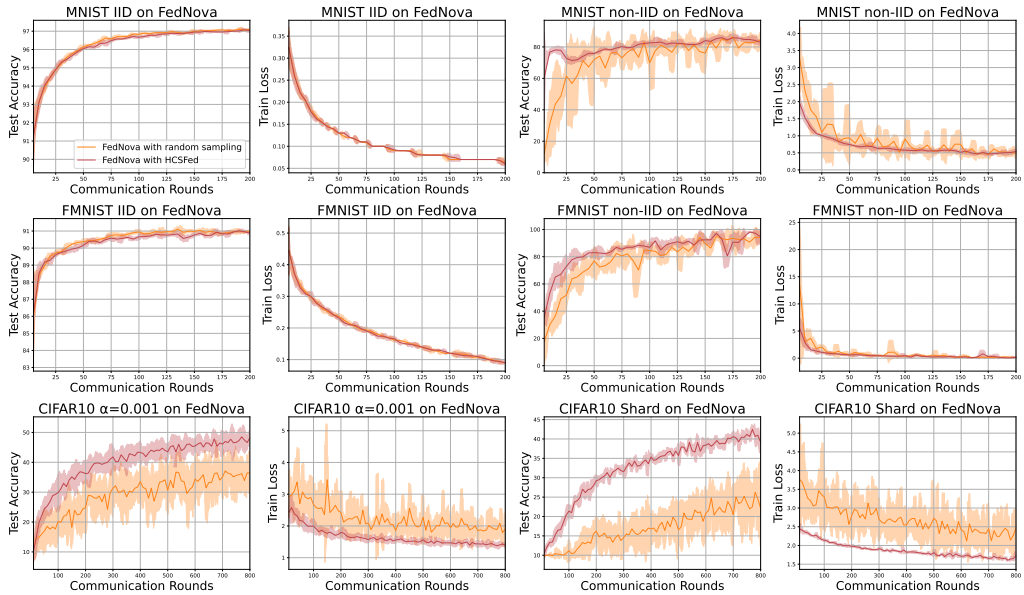


Figure 11: Results on the MNIST, FMNIST and CIFAR10 under FedNova. We compare  $\text{HCSFed}$  with simple random sampling, using a Dirichlet Distribution with  $\alpha = 0.001$  and Shard, setting parameters  $q = 0.1$ ,  $N = 100$ ,  $nSGD = 50$  for MNIST and FMNIST,  $nSGD = 80$  for CIFAR-10,  $\eta = 0.05$ ,  $B = 50$ .